Hirsch, J.G.; Castaños, O.; López-Peña, R.; Jiménez F., O.; López-Moreno, E.
Hartree-Fock description of spin systems

Disponible en: http://www.redalyc.org/articulo.oa?id=57028300008

Hartree-Fock description of spin systems

J.G. Hirsch, O. Castaños, R. López-Peña, and O. Jiménez F.
Instituto de Ciencias Nucleares, Universidad Nacional Autónoma de México,
Apartado Postal 70-543 México 04510 D.F.,
e-mail: hirsch@nucleares.unam.mx, ocasta@nucleares.unam.mx,
lopez@nucleares.unam.mx, and ofarias@nucleares.unam.mx

E. López-Moreno
Departamento de Física, Facultad de Ciencias, Universidad Nacional Autónoma de México,
Apartado Postal 70-542 México 04510 D.F.,
e-mail: elm@hp.fciencias.unam.mx

A mean-field treatment of a general spin Hamiltonian containing linear and quadratic terms is presented. The equivalence between atomic coherent states and Hartree-Fock states is explicitly demonstrated. The relevance of symmetry restoration is exhibited. Entanglement properties at the different phases are briefly discussed.

Keywords: Spin Hamiltonian; coherent state; Hartree-Fock; entanglement.

Se presenta un estudio de campo medio de un Hamiltoniano de un sistema de espines que contiene términos lineales y cuadráticos. Se muestra explícitamente la equivalencia entre los estados coherentes atómicos y los estados de Hartee-Fock. Se exhibe la releancia de la restauración de simetrías. Las propiedades de enredamiento en las diferentes fases del sistema se discuten brevemente.

Descriptores: Hamiltoniano de espines; estado coherente; Hartree-Fock; enredamiento.

PACS: 05.70.Fh; 03.65.Fd; 21.60.Fw; 42.50.Dv

1. Introduction

Systems formed of interacting spins have been subject of interest along decades, due both to their theoretical simplicity, and their usefulness as an approximate description of a large variety of quantum systems. For some of these systems, the interaction parameter strengths have recently been shown to be subject to experimental control, allowing the study of entanglement and phase transitions in a variety of situations.

The Lipkin nuclear model is simple enough to be solved exactly but it is yet non-trivial. For that reason, since it was established [1], it has been used to compare the behavior of many fermion approximation methods like for example the random phase approximation (RPA), the renormalized RPA and the self-consistent RPA [2].

The Lipkin model, as originally conceived, describes an extremely simplified nucleus as a system of fermions which can occupy two levels with the same degeneracy 2J+1, which are separated by an energy ϵ. Besides, the nucleons have residual interactions which scatters pairs of particles between the two levels without changing the particular degenerate states within the shells. The model has been also useful to describe two-species boson condensates, and other bosonic systems.

The model Hamiltonian is taken from [1,3] and it reads

$$H = \epsilon J_0 + \frac{\lambda}{2}\left(J_+^2 + J_-^2\right) + \frac{\gamma}{2}\left(J_+J_- + J_-J_+\right). \quad (1)$$

The λ-term annihilates pairs of particles in one level and creates pairs in the other level. The γ-term scatters one particle up while another is scattered down.

The angular momentum operators can be realized in terms of fermion creation $c_{\alpha m}^\dagger$ and annihilation operators $c_{\alpha m}$, satisfying $\{c_{\alpha m}, c_{\alpha' m'}^\dagger\} = \delta_{\alpha,\alpha'}\delta_{m,m'}$,

$$J_0 = \frac{1}{2}\sum_{m=0}^{2J}(c_{+m}^\dagger c_{+m} - c_{-m}^\dagger c_{-m}),$$

$$J_+ = \sum_{m=0}^{2J} c_{+m}^\dagger c_{-m}, \quad (2)$$

$$J_- = \sum_{m=0}^{2J} c_{-m}^\dagger c_{+m}.$$

The index $\alpha = +,-$ denotes the lower and upper single particle levels, with energies $\epsilon_\pm = \mp\epsilon/2$, ϵ being the energy spacing between levels, and m is the internal quantum number (*i.e.* the angular momentum projection) which varies between $0 \to 2J$ for each shell. These operators are the generators of the algebra of the SU(2) group. Hamiltonian (1) commutes with the operator J^2, and thus the Hamiltonian matrix breaks up into submatrices, each associated with a different value of J and of order $2J + 1$.

The same system can be visualized as consisting in two kind of bosons a, b, each with energies ϵ_a, ϵ_b, whose difference is $\epsilon_b - \epsilon_a = \epsilon$. The realization of the SU(2) algebra in the bosonic case is

$$J_0 = \frac{1}{2}(b^\dagger b - a^\dagger a), \quad J_+ = b^\dagger a, \quad J_- = a^\dagger b. \quad (3)$$

As it is usual, for simplicity only the case with maximum symmetry $N = 2J$ is considered. Exact eigenvalues and eigenvectors of the Hamiltonian H, Eq. (1), are obtained in the basis $\{|Nn\rangle\}$, with n varying from 0 to N, defined as

$$|Nn\rangle = \sqrt{\frac{(N-n)!}{N!(n)!}}\, J_+^n |N0\rangle. \qquad (4)$$

The state $|N0\rangle$ is the unperturbed ground state, i.e. the ground state when $\lambda = \gamma = 0$. In this case all the particles occupy the lowest single particle state. In the fermionic description it has the form $|N0\rangle = \prod_{m=0}^{N} c_{-m}^\dagger |\rangle$, and in the bosonic description $|N0\rangle = (1/\sqrt{N})(a^\dagger)^N |\rangle$, being $|\rangle$ in each case the appropriate bare vacuum.

Since the Hamiltonian (1) has non-vanishing matrix elements between states (4) with $n \to n, n \pm 2$ its eigenfunctions can be written in terms of linear combinations of states with even (e) or odd (o) values of n (e.g. the number of particle-hole pairs), namely:

$$|\alpha, e\rangle = \sum_{i=0}^{J} C_{i,e}^\alpha |N2i\rangle,$$
$$|\alpha, o\rangle = \sum_{i=0}^{J-1} C_{i,o}^\alpha |N2i+1\rangle. \qquad (5)$$

In this notation α is the eigenvalue-index, thus $|\alpha = 1, e\rangle$ and $|\alpha = 1, o\rangle$ are the lowest energy even and odd states, respectively, which can correspond to the ground and first excited states, as discussed below.

The lowest exact energies E_e and E_o, obtained by diagonalization in the basis of even- and odd- states, are presented in Fig. 1, as function of the Hamiltonian parameter strengths λ and γ, for N= 20 particles. They exhibit sudden changes in the slope along the phase transitions, which have been described in detail in Ref. 4.

Although both energy surfaces look very similar, there are crossings between them. The ground state of the system is an even or odd state for given interaction strengths, depending on which of them has the lowest energy. Their differences

are presented in the upper panel of Fig. 2. The projection in the $\lambda - \gamma$ plane is shown in the lower panel. The crossing points where both energies become degenerate over hyperbolae in the parameter space, whose analytical expressions are given in Ref. 4.

2. Hartree-Fock description

It is instructive to present in some length the application of the Hartree-Fock method to the generalized Lipkin model. In this section we follow the treatment of Ring & Schuck [5].

Given that Hamiltonian (1) is invariant under the permutation of the 2Ω states below or above the Fermi level, the most general Slater determinant which serves as a Hartree-Fock trial ground state is

$$|0\rangle = \prod_{m=0}^{N} a_{0m}^\dagger |\rangle, \qquad (6)$$

where $|\rangle$ is the "bare" particle vacuum, satisfying

$$c_{+m}|\rangle = 0, \qquad c_{-m}|\rangle = 0, \qquad (7)$$

and

$$|N0\rangle = \prod_{m=0}^{N} c_{-m}^\dagger |\rangle \qquad (8)$$

is the particle-hole vacuum, satisfying

$$c_{+m}|N0\rangle = 0, \qquad c_{-m}^\dagger |N0\rangle = 0, \qquad (9)$$

The Hartree-Fock state $|0\rangle$ is, by construction, the particle-hole vacuum of the new operators

$$a_{0m}^\dagger = \mu^* c_{-m}^\dagger - \nu c_{+m}^\dagger ,$$
$$a_{1m}^\dagger = \nu^* c_{-m}^\dagger + \mu c_{+m}^\dagger , \qquad (10)$$

where 0 and 1 denote the new lower and upper levels, and coefficients μ and ν satisfy the condition $|\mu|^2 + |\nu|^2 = 1$.
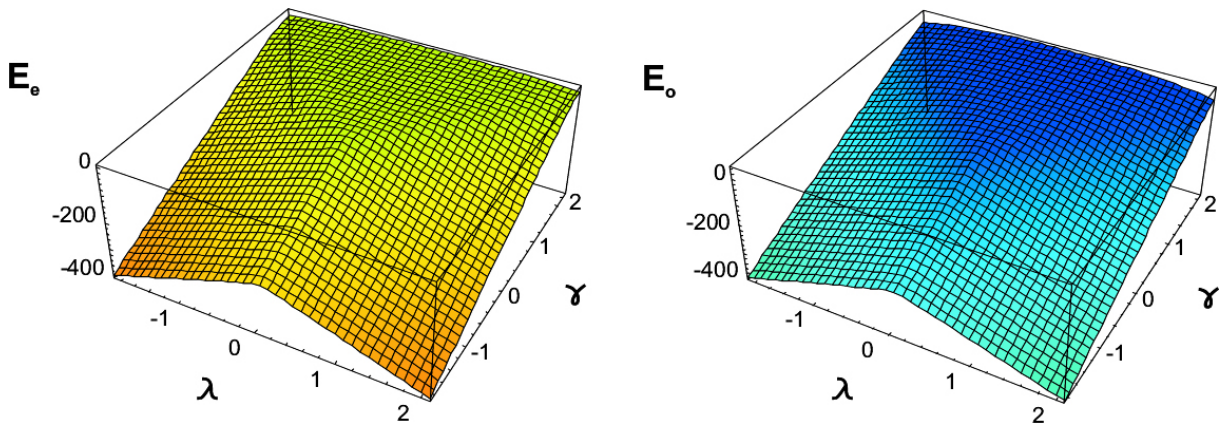

FIGURE 1. The exact even and odd lowest energies.

The Thouless' theorem [5] allows the direct association of the Hartree-Fock (6) and coherent [4] states:

$$|0\rangle = \frac{|\zeta\rangle}{\langle\zeta|\zeta\rangle}, \tag{11}$$

with the spin coherent states defined by [6]

$$|\zeta\rangle = \exp(\zeta J_+)|J, -J\rangle, \tag{12}$$

where $\zeta = \tan(\theta/2)\exp(i\phi)$ and J is associated with the number of particles.

Using the inverse relations

$$\begin{aligned} c_{-m}^\dagger &= \mu a_{0m}^\dagger + \nu a_{1m}^\dagger, \\ c_{+m}^\dagger &= -\nu^* a_{0m}^\dagger + \mu^* a_{1m}^\dagger, \end{aligned} \tag{13}$$

and the Wigner parametrization of the SU(2) transformations

$$\begin{aligned} \mu &= e^{-i(\psi+\phi)/2}\cos(\theta/2), \\ \nu &= -e^{-i(\psi-\phi)/2}\sin(\theta/2), \end{aligned} \tag{14}$$

the quasispin operators can be written in the new basis

$$\begin{aligned} J_+ &= e^{i\phi}\left(-\sin\theta K_0 + \frac{1}{2}(1+\cos\theta)e^{i\psi}K_+ \right. \\ &\qquad\qquad \left. -\frac{1}{2}(1-\cos\theta)e^{-i\psi}K_-\right), \\ J_0 &= \cos\theta K_0 + \frac{1}{2}\sin\theta\left(e^{i\psi}K_+ + e^{-i\psi}K_-\right), \quad (15) \\ J_- &= e^{-i\phi}\left(-\sin\theta K_0 - \frac{1}{2}(1-\cos\theta)e^{i\psi}K_+ \right. \\ &\qquad\qquad \left. +\frac{1}{2}(1+\cos\theta)e^{-i\psi}K_-\right), \end{aligned}$$

where we have introduced the new quasispin operators

$$\begin{aligned} K_0 &= \frac{1}{2}\sum_{m=0}^{2\Omega}(a_{1m}^\dagger a_{1m} - a_{0m}^\dagger a_{0m}), \\ K_+ &= \sum_{m=0}^{2\Omega} a_{1m}^\dagger a_{0m}, \quad (16) \\ K_- &= \sum_{m=0}^{2\Omega} a_{0m}^\dagger a_{1m}. \end{aligned}$$

Hamiltonian (1) in the new basis reads

$$\begin{aligned} H = & \left\{\epsilon\cos\theta + \frac{\lambda}{2}\sin^2\theta\cos(2\phi) - \frac{\gamma}{2}\left(1+\cos^2\theta\right)\right\}K_0 \\ & + \frac{1}{2}\sin\theta\left\{\epsilon - \lambda\left[\cos(2\phi)\cos\theta + i\sin(2\phi)\right] + \gamma\cos\theta\right\}e^{i\psi}K_+ \\ & + \frac{1}{2}\sin\theta\left\{\epsilon - \lambda\left[\cos(2\phi)\cos\theta - i\sin(2\phi)\right] + \gamma\cos\theta\right\}e^{-i\psi}K_- \\ & + \sin^2\theta\left\{\lambda\cos(2\phi) + \gamma\right\}K_0^2 \\ & - \sin\theta\left\{\lambda\left[\cos(2\phi)\cos\theta + i\sin(2\phi)\right] + \gamma\cos\theta\right\}e^{i\psi}K_+ K_0 \\ & - \sin\theta\left\{\lambda\left[\cos(2\phi)\cos\theta - i\sin(2\phi)\right] + \gamma\cos\theta\right\}e^{-i\psi}K_0 K_- \\ & - \frac{1}{2}\left\{\sin^2\theta\cos(2\alpha) - \gamma\left(1+\cos^2\theta\right)\right\}K_+ K_- \\ & + \frac{1}{4}\left\{\lambda\left[\cos(2\phi)\left(1+\cos^2\theta\right) - 2i\sin(2\phi)\cos\theta\right] - \gamma\sin^2\theta\right\}e^{2i\psi}K_+^2 \\ & + \frac{1}{4}\left\{\lambda\left[\cos(2\phi)\left(1+\cos^2\theta\right) + 2i\sin(2\phi)\cos\theta\right] - \gamma\sin^2\theta\right\}e^{-2i\psi}K_-^2. \end{aligned} \tag{17}$$

In the above expression the Hamiltonian is written in normal order. Using the properties of the Hartree-Fock ground state

$$K_0|0\rangle = -\Omega|0\rangle, \quad K_-|0\rangle = 0, \tag{18}$$

it is direct to evaluate the expectation value of the Hamiltonian in this state,

$$\langle 0|H|0\rangle = \frac{\langle\zeta|H|\zeta\rangle}{\langle\zeta|\zeta\rangle} = E(\theta, \phi). \tag{19}$$

For given values of the Hamiltonian parameters, it represents the *classical energy surface*. After making a shift and a magnification, the expectation value of the Hamiltonian between coherent states can be written as [3]
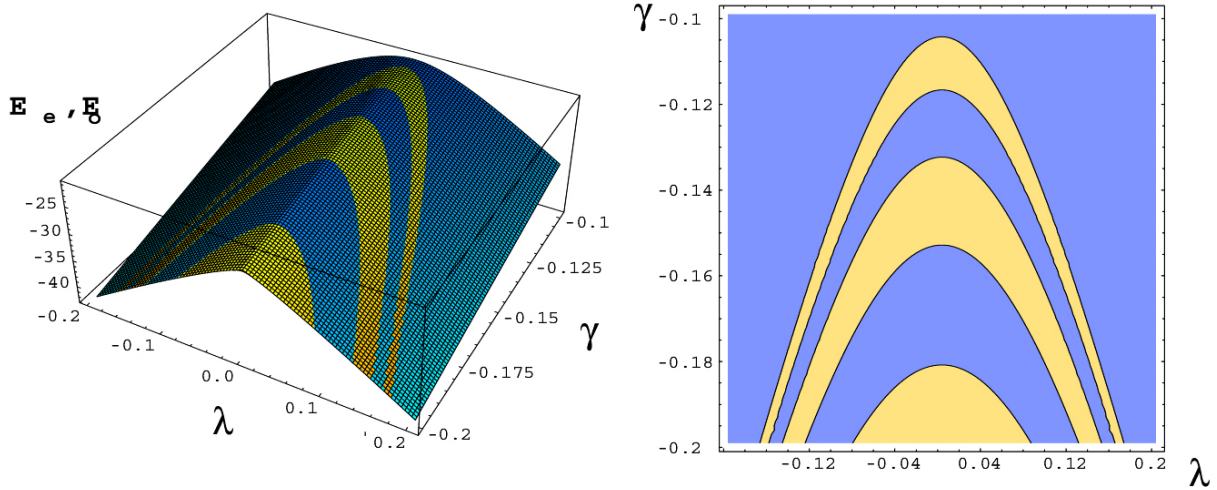
FIGURE 2. Differences between the exact even and odd lowest energies (left panel) and their projection in the $\lambda - \gamma$ plane (right panel).

$$\mathcal{E}(\theta, \phi) = \frac{\langle \zeta | H | \zeta \rangle - \gamma j}{\omega j},$$

$$= -2 \cos \theta + \gamma_x \sin^2 \theta \cos^2 \phi$$
$$+ \gamma_y \sin^2 \theta \sin^2 \phi , \quad (20)$$

where the parameters γ_x and γ_y are defined by

$$\gamma_x = \frac{2j-1}{2\omega}(\gamma + \lambda), \quad \gamma_y = \frac{2j-1}{2\omega}(\gamma - \lambda) . \quad (21)$$

From here on, a variational treatment follows, which defines the numbers (θ_0, ϕ_0) which minimize $E(\theta, \phi)$ [4]. They are

$$\sin(2\phi_0) = 0, \quad \lambda \cos(2\phi_0) = -|\lambda|,$$
$$\cos(\theta_0) = 0, \quad \text{if} \quad |\gamma - |\lambda|| < \epsilon/(2\Omega - 1), \quad (22)$$
$$\cos(\theta_0) = \epsilon/((2\Omega - 1)(\gamma - |\lambda|)) \quad \text{otherwise.}$$

To describe the one-body excitation at the Hartree-Fock level, we approximate the two-body operators as

$$K_\alpha K_\beta \rightarrow \langle 0 | K_\alpha | 0 \rangle K_\beta + K_\alpha \langle 0 | K_\beta | 0 \rangle, \quad (23)$$
$$\alpha, \beta = 0, +, -,$$

which implies

$$K_0^2 \rightarrow -2\Omega K_0, \qquad K_0 K_- \rightarrow \Omega K_-,$$
$$K_+ K_0 \rightarrow -\Omega K_+, \qquad K_+ K_- \rightarrow 0, \quad (24)$$
$$K_+^2 \rightarrow 0, \qquad K_-^2 \rightarrow 0.$$

The ground state energy (20) was already computed, and must be subtracted from this expression, which is only valid as an approximation for the excitation energies.

We obtain

$$H_{HF} = E_0 + h_{11}(K_0 + \Omega) + h_{20}(K_+ - K_-)$$
$$= E_0 + \mathcal{E}(K_0 + \Omega), \quad (25)$$

because

$$h_{20} = \frac{1}{2} \sin \theta_0 \left(\epsilon + (2\Omega - 1)(\gamma - |\lambda|) \cos \theta_0 \right) = 0, \quad (26)$$

due to the variational condition satisfied by E_0. Also

$$\mathcal{E} = \gamma - \left(2\Omega - \frac{1}{2} \right)(\gamma - |\lambda|) - \frac{1}{2} \frac{\epsilon^2}{(2\Omega - 1)^2(\gamma - |\lambda|)}$$
$$= - \left(2\Omega - \frac{\sin^2 \theta_0}{2} \right)(\gamma - |\lambda|) + \gamma. \quad (27)$$

2.1. The simplest Hartree-Fock approximation

We can build the Hartree-Fock Hamiltonian directly from (1), applying the same criteria to the original operators J_α

$$J_\alpha J_\beta \rightarrow \langle 0 | J_\alpha | 0 \rangle J_\beta + J_\alpha \langle 0 | J_\beta | 0 \rangle, \quad (28)$$
$$\alpha, \beta = 0, +, -.$$

From the properties of the HF vacuum (18), it is direct to obtain

$$\langle 0 | J_+ | 0 \rangle = \Omega e^{i\phi} \sin \theta,$$
$$\langle 0 | J_- | 0 \rangle = \Omega e^{-i\phi} \sin \theta, \quad (29)$$
$$\langle 0 | J_0 | 0 \rangle = -\Omega \cos \theta.$$

The approximate Hartree-Fock Hamiltonian $\tilde{H}_{HF}$ has now only one-body terms in the rotated basis, and reads:

$$\tilde{H}_{HF} = \left(\epsilon \cos \theta - 2\Omega \sin^2 \theta (\lambda \cos(2\phi) + \gamma) \right) K_0$$
$$+ \frac{1}{2} \sin \theta \left(\epsilon + 2\Omega \cos \theta (\lambda \cos(2\phi) + \gamma) \right)$$
$$\times (K_+ e^{i\psi} + K_- e^{-i\psi}) \quad (30)$$
$$+ i\Omega\lambda \sin(2\phi) \sin \theta (K_+ e^{i\psi} - K_- e^{-i\psi})$$

When evaluating the Hartree-Fock energy $\tilde{E}_{HF}$, care must me taken to avoid double counting the contribution of the two body terms, which were already averaged. It introduces a factor 1/2 in the potential energy [5, 7]:

$$\tilde{E}_{HF} = \langle T \rangle + \frac{1}{2}\langle U \rangle$$

$$= \epsilon\cos\theta\langle K_0\rangle - \frac{1}{2}2\Omega\sin^2\theta(\lambda\cos(2\phi) + \gamma)\langle K_0\rangle$$

$$= -\epsilon\Omega\cos\theta + \Omega^2\sin^2\theta(\lambda\cos(2\phi) + \gamma) \qquad (31)$$

Notice that the averaging procedure erased the fermionic content of the quasispin operators, which now contribute with a factor $(2\Omega)^2$ instead of $2\Omega(2\Omega-1)$ as in (20). Also the constant $\gamma\Omega$ is missing, because Hamiltonian (1) was not written in normal order before using the Hartree-Fock approximation.

The variational procedure gives the values $(\tilde{\theta}_0, \tilde{\phi}_0)$ which minimize $\tilde{E}_{HF}$. They agree with Eq. (22), and with the results reported in Ref. 4, in the limit $2\Omega \gg 1$.

3. Projected Hartree Fock states

Although the Hartree-Fock energy reproduces quite accurately the exact ground state energy when the number of particles becomes large, it has a significant flaw: mixes states with different parity, violating the *parity symmetry* of the Hamiltonian, associated with the existence of even and odd eigenstates, Eq. (5).

Hartree-Fock states with good parity properties can be built as even and odd spin coherent states given by

$$|\zeta\rangle_{\pm} = \frac{1}{\sqrt{2(1 \pm (\cos\theta)^{2J})}}(|\zeta\rangle \pm |-\zeta\rangle). \qquad (32)$$

The expectation value of the Hamiltonian between the even (+) and odd (−) spin coherent states takes the form

$$\varepsilon_{\pm}(\theta,\phi) = \frac{\pm\langle\zeta|H|\zeta\rangle_{\pm} - \gamma J}{\omega J},$$

$$= \varepsilon(\theta,\phi)F_{\pm}(\theta, J) \mp (\gamma_x + \gamma_y)G_{\pm}(\theta, J), \qquad (33)$$

where the functions F, G are given by the expressions

$$F_{\pm}(\theta, J) = \frac{1 \pm (\cos\theta)^{2J-2}}{1 \pm (\cos\theta)^{2J}},$$

$$G_{\pm}(\theta, J) = \frac{(\sin\theta)^2(\cos\theta)^{2J-2}}{1 \pm (\cos\theta)^{2J}}. \qquad (34)$$

The same shift and magnification are chosen for the three energy surfaces to allow a simple comparison between them. When $J \to \infty$, the functions $F_{\pm}$ go to the unity, and functions $G_{\pm}$ go to zero.

The parity projected Hartree-Fock energies are obtained by performing *variation after projection*, which in general is a very cumbersome procedure, but in this case is numerically simple. The resultant energy surfaces are displayed in Fig. 3. The crossing between the even and odd surfaces is clearly visible in the plot, whose projection on the $\gamma - \lambda$ plane is presented in the lower panel. The comparison with the exact energies shown in Fig. 2 exhibit the excellent quality of the parity projected Hartree-Fock energies. The first degeneracy region, the hyperbola which characterize the crossing between even and odd-parity states, is correctly reproduced. It is associated with a first order phase transition present in the system, which the Hartree-Fock state does not detect, but is clearly revealed when parity projection is introduced.

4. Entanglement in the different phases

A relevant property of many particle systems is their *entanglement*, which quantifies the correlations between different parts of the whole quantum system. This quantity is very sensitive to the ground state wave function. This section briefly introduces a relevant bipartite entanglement measure, the von Neumann entropy. The close relationship between entanglement and phase transitions is exhibited.
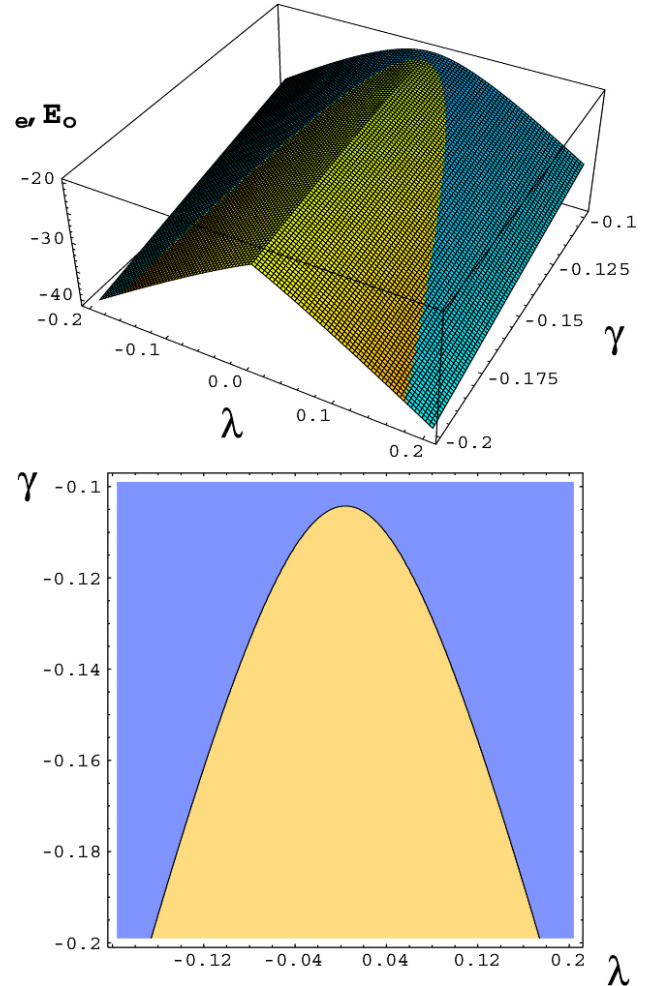

FIGURE 3. Even and odd energy surfaces obtained with parity projected Hartree-Fock states.
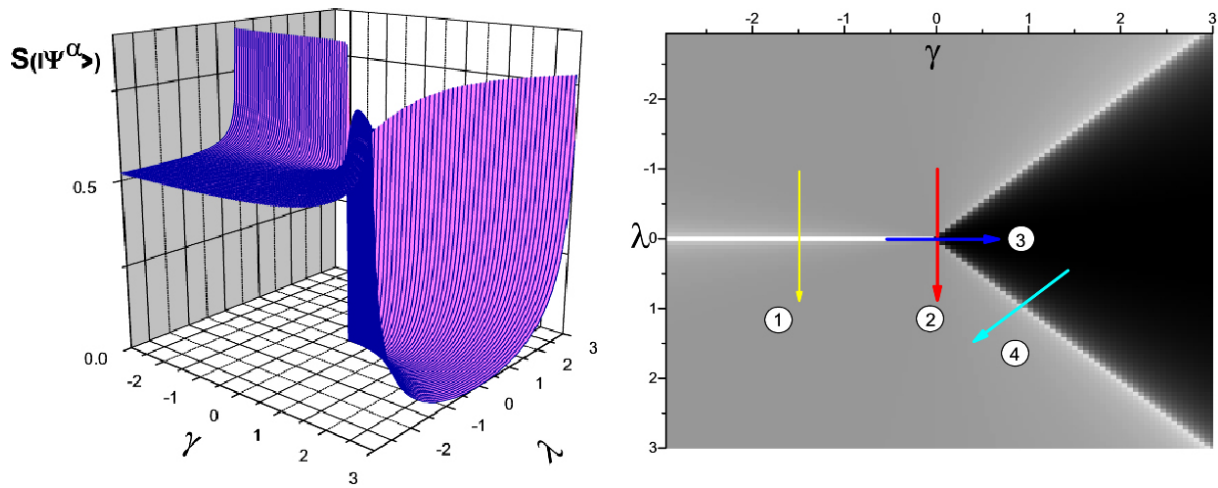
FIGURE 4. Von Neumann Entropy as a function of the parameters of the system (left panel). In the right hand side a gray level map of the same entropy shows the trajectories in the $\gamma - \lambda$ plane.
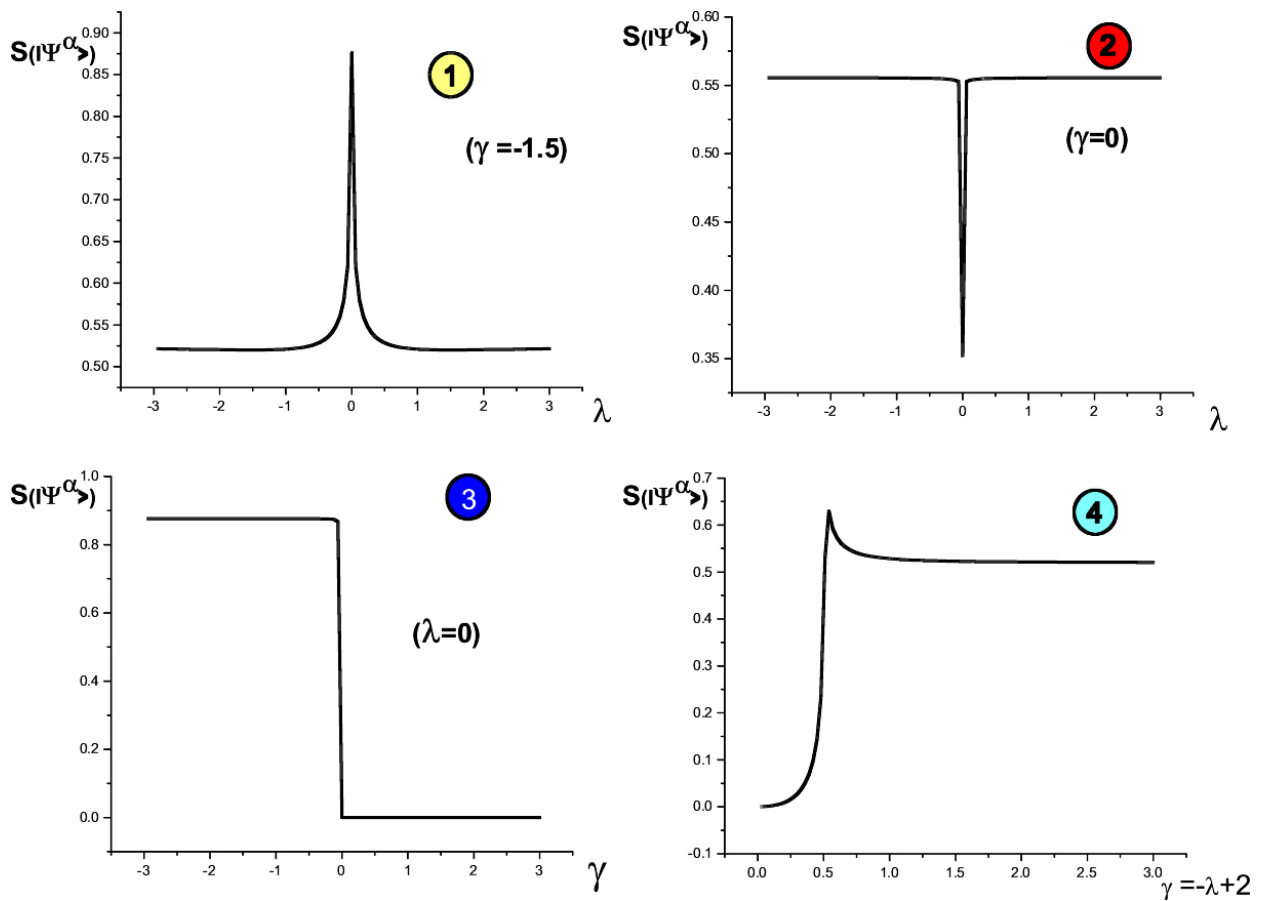

FIGURE 5. Entropy calculated along the trajectories in the $\gamma - \lambda$, as presented in Ref. 4.

Knowing the exact ground state of the system it is possible to build the reduced density matrix associated with a partition of the N-particle system into two subsystems. For the most general SU(2) state with constant J:

$$|\Psi^\alpha\rangle = \sum_M a_M^\alpha |J, M\rangle,$$

with $N = 2J$ particles, the two subsytems will have $2j_1$ and $2j_2$ particles, with $j_1 + j_2 = J$. A particular state $|J, M\rangle$ can be decomposed as

$$|J, M\rangle = \sum_{m_1 = -j_1}^{j_1} P^{\frac{1}{2}}(m_1, M)|j_1, m_1\rangle|j_2, M - m_1\rangle, \quad (35)$$

with the coeficients $P^{\frac{1}{2}}$ being the Clebsch Gordan coeficients.

In order to estimate the bipartite entanglement the reduced matrix elements [8]

$$\rho_{\mu,\nu}^{(1)}(|\Psi^\alpha\rangle)$$

$$= \sum_{l = -j_2}^{j_2} a_{l+\mu}^\alpha a_{l+\nu}^{*\alpha} P^{1/2}(\mu, l+\mu) P^{1/2}(\nu, l+\nu) \quad (36)$$

must be evaluated

For the LMG model, the coefficients a_M^α corresponding to the ground state are $C_{M,e/o}^\alpha$ in Eq. (5). They depend on the Hamiltonian parameters γ, λ. The exact Von Neumann entropy is calculated as in Ref. 8, exhibiting an extreme sensibility to phase transitions.

For small number of particles, crossing between levels dominates the behavior of the *surface of entanglement* but, as the number of particles increases, the collective behavior starts playing a determinant role, and the separatrix of the system can be recovered by analyzing the bipartite entanglement of the system.

In Fig. 4 and 5 results for N=50 particles are presented, employing the partition (25,25). While the entanglement is dependent of the partition used, the general behavior in the different phases is similar for any of them. In those parameter regions where the coherent state has its minimum for $\theta_c = 0$ the von Neumann entropy is zero. On the opposite side, it has a maximum value in the most deformed regions.

In the right hand side of Fig. 4 different trajectories in the $\gamma - \lambda$ plane are presented. Along them phase transitions take place when the separatrix of the system is crossed. The entanglement entropy is displayed in Fig. 5 for this trajectories. Different kinds of finite discontinuities in the entanglement are observed, which can be related with phase transition of various orders, according to the classification of Ref. [4].

5. Conclusions

The LMG model describes a spin system with non-linear interactions. It displays a very rich behavior when the two-body interaction strengths are varied. The exact quantum solutions exhibit both crossings between levels with different parities, and anticrossings (level repulsion) between states with the same parities. The exact energy surfaces show sudden changes in their slopes for certain parameter values, which were associated with classical phase transitions. Standard, even and odd coherent states allowed the construction of the respective energy surfaces. For the standard energy surface, the catastrophe formalism allowed for a complete classification of the critical points. Some of them belong to the bifurcation and Maxwell sets, and define the separatrix of the model.

Even and odd energy surfaces were shown to closely reproduce the exact quantum behavior of the ground and first excited states, and their degeneracy. Inside the parameter region between the hyperbolae there are no crossings between energy levels, whereas in the exterior part, degeneracy is present. It was also shown that the von Neumann entropy of the system exhibits sudden changes which are closely related to the phase transitions.

Acknowledgments

1. H.J. Lipkin, N. Meshkov, and A.J. Glick, *Nucl. Phys.* **62** (1965) 188, 199, 211.

2. J.G. Hirsch, O. Civitarese, and M. Reboiro, *Phys. Rev.* **C60** (1999) 24309.

3. O. Castaños, E. López-Moreno, and R. López-Peña, *Rev. Mex. Fis.* **49S(4)** (2003) 15.

4. O. Castaños, R. López-Peña, J.G. Hirsch, and E. López-Moreno, *Phys. Rev. B* **72**, 012406 (2005); *ibid*, *Phys. Rev. B* **74** (2006) 104118..

5. P. Ring and P. Schuck, *The Nuclear Many-Body Problem*, (Springer-Verlag, New York 1980).

6. F.T. Arecchi, E. Courtens, R. Gilmore, and H. Thomas, *Phys. Rev. A* **6** (1972) 2211.

7. A. Bohr and B.R. Mottelson, *Nuclear Structure* V II, (Benjamin, Reading, Mass. 1975).

8. J.I. Latorre, R. Orús, E. Rico, and J. Vidal, *Phys. Rev. A* **71** (2005) 064101.